



Quantum-inspired evolutionary optimization of SLMoS₂ two-phase structures

Wacław Kuś¹ , Adam Mrozek^{2*} 

¹ Silesian University of Technology, Gliwice, Poland.

² AGH University of Science and Technology, Krakow, Poland.

Abstract

The paper focuses on applying a Quantum Inspired Evolutionary Algorithm to achieve the optimization of 2D material containing two phases, 2H and 1T, of Molybdenum Disulphide (MoS₂). The goal of the optimization is to obtain a nanostructure with tailored mechanical properties. The design variables describe the shape of inclusion made from phase 1T in the 2H unit cell. The modification of the size of the inclusions leads to changes in the mechanical properties. The problem is solved with the use of computed mechanical properties on the basis of the Molecular Statics approach with ReaxFF potentials.

Keywords: quantum-inspired evolutionary algorithm, optimization, nanostructure, two-phase SLMoS₂, molecular dynamics, molecular statics, atomic potential, ReaxFF, material properties

1. Introduction

Optimization plays an important role in the design and numerical modelling of existing macro and nanomechanical systems. By appropriately formulating the optimization problems, including the objective function, constraints, and design variables, it is possible to obtain new solutions with better tailored mechanical properties which are less energy-consuming, more durable or lighter. A special case of the optimization problems associated with materials science is the design of new two-dimensional (2D) nanomaterials and nanostructures.

2D materials can be classified as periodic, flat lattices made of replicated stable configurations of atoms. The importance of 2D in the development of modern electronic and optoelectronic devices, as well as sensors and sophisticated composites, is crucial (Jiang, 2015; Li et al., 2015). The last decade has seen an abundance of studies on the carbon-based graphene

allotropes, revealing their unique mechanical, thermal and electronic properties (Cranford & Buehler, 2011; Enyashin & Ivanovskii, 2011; Maździarz et al., 2018; Mrozek & Burczyński, 2018; Park et al., 2012; Peng et al., 2012). Other examples of monoatomic 2D materials, made up of graphene-like honeycomb lattices, are allotropes called bismuthene, germanene, silicene and stanene, based on bismuth, germanium silicon and tin atoms respectively. On the other hand, similar hexagonal flat structures can be made of atoms of different elements, like boron nitride and single-layered molybdenum disulfide (SLMoS₂). The scientific work of the authors has been related to the latter (Mrozek, 2019; Kuś et al., 2022).

Several methods of searching for new stable configurations of flat as well as three-dimensional nanostructures have been developed over the last few years. Most of these algorithms combine non-classical optimization techniques with simulations on the atomic-level, like

*Corresponding author: amrozek@agh.edu.pl

ORCID ID's: 0000-0001-7616-6881 (W. Kuś), 0000-0001-8309-6156 (A. Mrozek)

© 2022 Authors. This is an open access publication, which can be used, distributed and reproduced in any medium according to the Creative Commons CC-BY 4.0 License requiring that the original work has been properly cited.

Molecular Dynamics (MD) or Molecular Statics (MS), or even quantum levels like CALYPSO (Wang et al., 2010), an approach which combines Particle Swarm Optimization (PSO) and *ab initio* calculations.

The authors of this work previously successfully implemented various bio-inspired algorithms: from the Artificial Immune System (AIS) and PSO, to Evolutionary and Memetic Algorithms (Kuś et al., 2016, 2022; Mrozek et al., 2010, 2015). These routines have been linked with MS and MD solvers and engaged in processes of searching for small, three-dimensional, aluminium clusters, new stable graphene allotropes, and other carbon-based 2D materials with predefined mechanical properties. This paper summarizes the next stage in the development of the author's own methods of optimization and searching for new, stable nanostructures and further research on various 2D materials.

The optimization problem was formulated as minimizing the difference between the given material parameters and the values for a given vector of design variables. The closer the material parameters are to the set ones, the smaller the objective function's value. The optimization algorithm allows the easy formulation of the optimization problem due to the coding of the design variables. An attempt was made to solve a similar problem with the use of an evolution algorithm based on floating point design variables representation, but it required more calculations of the objective function than the proposed quantum-based approach.

The quantum-inspired evolutionary algorithm, the structure of the SLMoS₂, the ReaxFF atomic potential and the formulation of the optimization problem are described and explained in the following sections. The article ends with an analysis and discussion of the obtained results. The mechanical properties of the optimized two-phase atomic structures were verified during Molecular Dynamics based tensile tests.

2. Quantum-inspired evolutionary algorithm

To solve optimization problems, algorithms based on classical optimization methods using the gradient of the objective function are used frequently, as well as global methods based on biological phenomena (Burczyński et al., 2020). Another group of global optimization methods are algorithms inspired by quantum phenomena implemented and run on classical computers. These algorithms have been under development and modifications for two decades, and their applications are limited to common test problems (Han & Kim, 2002). The most important distinguishing feature of quantum-inspired algorithms is the representation of design variables using qubits. In classi-

cal computers, data is encoded with bits of 0–1 values, with a qubit being the equivalent of a bit in quantum computers. The qubit value also takes the 'pure value' 0 or 1 at the time of measurement, while during data processing, the qubit has a value often represented as one of the points in the Bloch sphere (Lahoz-Beltra, 2016) (Fig. 1a).

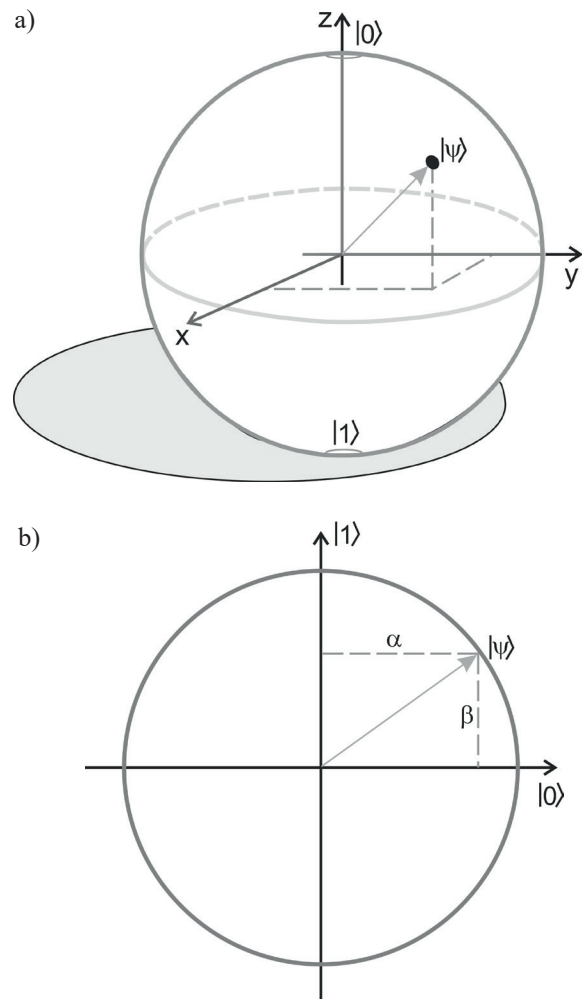


Fig. 1. Qubit represented on a Bloch sphere (a) and qubit representation on a circle (b)

The position can be defined by a vector containing two complex numbers. During data processing, this vector can change its values, while at the time of reading or measuring the qubit value, its value changes to one of the positions marked as $|0\rangle$ and $|1\rangle$. The value during the measurement is determined by the values of the qubit vector determining the probability of reaching the value 0 or 1, it may also depend on the phenomenon of qubits entanglement. In quantum-inspired algorithms, the position description using complex numbers is often abandoned in favour of real numbers, and the qubit value may be presented as a point on a circle or even on a segment of a circle (Fig. 1b). Data representation

with the use of qubits forces changes to optimization algorithms, individual operations of changing the design variables in subsequent iterations of the algorithm must take into account phenomena typical for qubits. The values of the design variables take values after reading individual qubits. However, the value of the objective function can still be determined in a traditional way. The representation of qubits using two real parameters is used in the paper. The qubit can be visualised as a circle in Figure 1b. The value of qubit during measurement can be either 0 or 1, as in the case of qubit state representation with complex numbers. The QEA algorithm operates in each of the steps on many solutions written in qubit vectors. The qubits determine the values of design variables values. The scheme of the QEA algorithm is shown in Figure 2. The presented algorithm is based on previously known solutions (Han & Kim, 2002; Lahoz-Beltra, 2016; Silveira et al., 2017; Zhang, 2011).

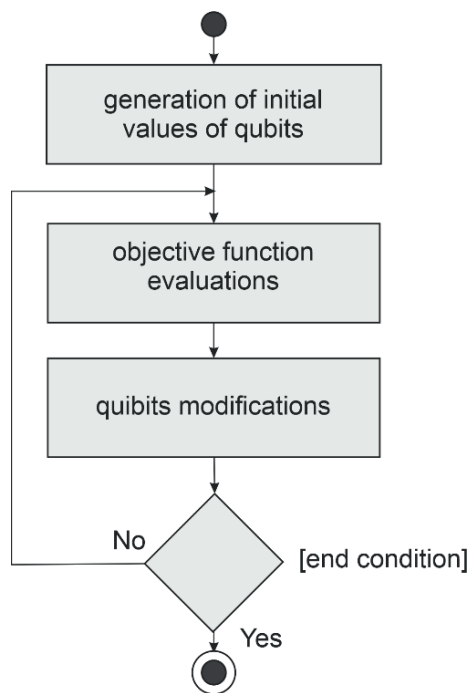


Fig. 2. QEA algorithm flowchart

First, a starting population is created containing qubits in the Hadamard state with a probability of 1 or 0 states after measurement equal to 50%, then each qubit is rotated by a random angle value. The algorithm uses an approach in which each of the qubits can take values defined by the real numerical values of two parameters. The qubit rotation is performed with the use of a typical quantum gate. In the next step, it is necessary to calculate the value of the objective function for each qubit vector that determines the values of the design variables. For this purpose, it is first necessary to measure the

values represented by each of the qubits (it should be remembered that the parameters of the qubit determine the probability it takes from a value of 1 or 0 during the measurement). After measurements are made, the bits are converted into the values of the design variables. The next stage of QEA consists in modifying the values of individual qubits with the use of mechanisms typical for evolutionary algorithms – mutations, rotation gates, as well as selection based on the value of the objective function specified for individual qubit vectors. The selection operator typical for the evolutionary algorithm is replaced in QEA with a similar to Particle Swarm Optimization operation where the qubits states are influenced by the best solution. Figure 3 illustrates qubits and the change of their value depending on the best solution qubit value, the modifications are introduced as rotations toward the best solution qubit position.

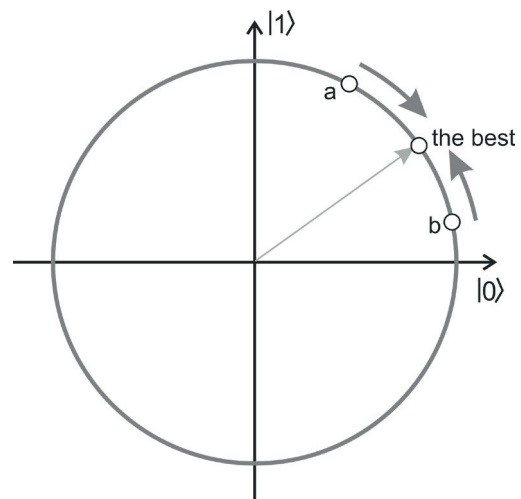


Fig. 3. The modification of qubits on the base of the best solution qubit

3. Two phase MoS_2 modelling

The SLMoS_2 has two stable polymorphs, usually called 2H and 1T, which can exist simultaneously, creating complex heterostructures. As presented in Figure 4, the most common 2H phase of the SLMoS_2 , similar to graphene, has a hexagonal honeycomb-like lattice. Despite the fact that SLMoS_2 is usually considered as a 2D material, it is composed of three atomic layers: a single central plane of Mo atoms is symmetrically covered by two layers of S atoms, with stacking sequence A–B–A. Each elementary unit cell contains a single Mo atom and two sulfur atoms. The replication of the unit along the armchair and zigzag directions results in the creation of a periodic lattice where each Mo atom is surrounded by the six sulfur nearest-neighbours.

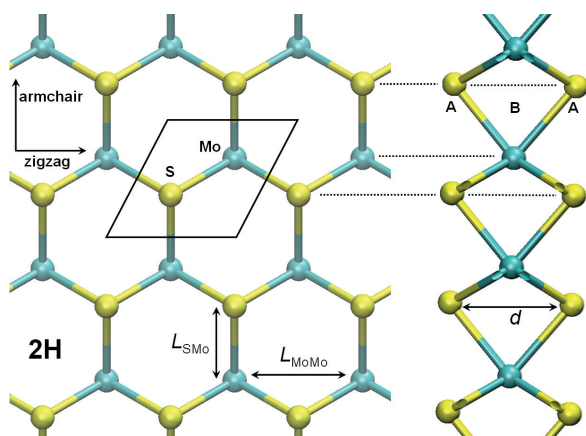


Fig. 4. SLMoS₂ 2H lattice

The main difference between the 2H and 1T phases is the stacking scheme of the outer layers (A–B–C instead of A–B–A). The one layer of sulfurs is shifted by half of the distance of the nearest-neighbour pairs S–Mo and Mo–Mo, denoted respectively by L_{SMo} and L_{MoMo} . Thus, the S atoms are placed in the centre of the hexagonal lattice created by the other two layers (Fig. 5).

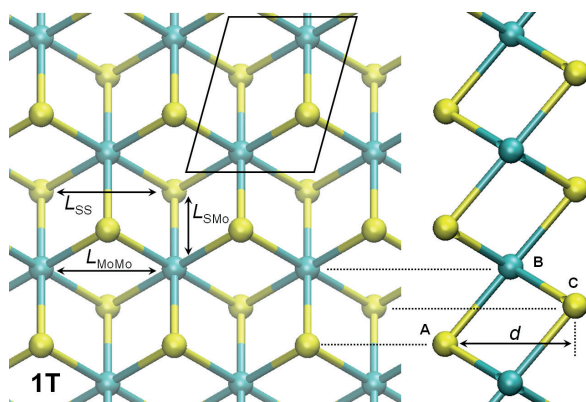


Fig. 5. SLMoS₂ 1T lattice

The structural and mechanical properties of the pristine SLMoS₂ lattices depend on the investigation methods adopted: experimental approaches, *ab initio* quantum calculations, MD and MS simulations with proper atomic potential. Distances L_{SMo} and L_{MoMo} , estimated using the DFT method by Xiong & Cao (2015) are equal to 2.408 Å and 3.181 Å, respectively, while the same parameters obtained during MD simulations, varies from 2.398 Å and 3.065 Å (Stillinger–Weber potential) to 2.444 Å 3.167 Å in the case of ReaxFF interaction model. Analogically, the effective thickness of the SLMoS₂, i.e. the distance between outer sulfur layers (d) varies from 3.114 Å (DFT) to 3.242 Å (ReaxFF). An exhaustive juxtaposition of the lattice parameters of the SLMoS₂ is also available in a paper by Mrozek (2019).

As already stated and reported by Lin et al. (2014), both 2H and 1T phases of SLMoS₂ can occur concurrently. However, the symmetry properties of the two described types of lattices restrict possible stable combinations and shapes of them to equilateral triangular or hexagonal geometries (Mortazavi et al., 2016).

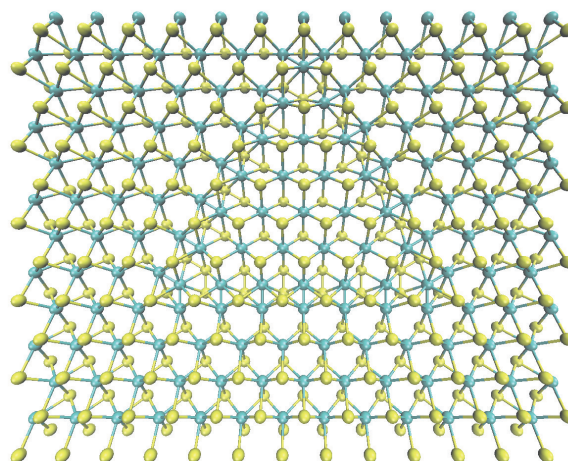


Fig. 6. SLMoS₂ heterostructure: triangular 1T inclusion, surrounded by 2H phase

An example of a combined SLMoS₂ triangular heterostructure, used in this work and similar to the one presented in the paper by (Mortazavi et al., 2016), is shown in Figure 6. Such an arrangement allows the imposition of periodic boundary conditions in the zigzag and armchair directions (compare Figure 6 with Figures 12 and 13, respectively) and a convenient parameterization of the geometry, as shown in Figures 7, 9 and 10.

ReaxFF potential

The reality, efficiency and precision of the performed nanoscale simulations are defined by the applied model of interatomic interactions. Such a model, called atomic potential, describes neighborhood-dependent potential energy of a whole atomic system, thus determining the forces acting between the atoms.

Unfortunately, the most accurate approach: *ab initio* calculations (Liang et al., 2009, 2012; Xiong & Cao, 2015), are not the optimal choice for geometrical optimization, where many independent simulations have to be solved in each iteration of the algorithm, mainly due to the high computational cost. However, in the case of discrete atomic models of the SLMoS₂ (as shown in Figures 4–6), methods of particle mechanics, like Molecular Dynamics, Molecular Statics (Buczyński et al., 2010) or even Conjugated Gradient-based energy minimization algorithms (Nakano, 1997) can be successfully used. Both of these methods engage atomic

potentials to handle atomic interactions with different degrees of accuracy.

The simplest, popular many-body and neighborhood-dependant potentials applied to modeling MoS₂ materials are based on the Stillinger–Weber and Reactive Empirical Bond Order (REBO) models, usually equipped with sets of parameters fitted to describe the behavior of a certain type of atoms in given conditions, and not all, but only selected spatial configurations and types of bondings.

Previous research by Mrozek (2019) have revealed that two available parameterizations of Stillinger–Weber (Liang et al., 2012; Kandemir et al., 2016) and REBO (Liang et al., 2009, 2012) potentials, although computationally efficient, are suitable for simulating 1T phase of SLMoS₂. Both approaches failed during the estimation of the mechanical properties of 1T lattice under small deformations. Additionally, the 1T to Body Centered Cell phase transition preceding the final damage mechanism was artificially introduced by an improperly parameterized potential.

As a trade-off between the accuracy of MS/MD simulations and computational time, the Reactive Force Fields model (ReaxFF) developed by van Duin et al. (2001) and Chenoweth et al. (2008), one of the most sophisticated and complex approaches and directly based on the data from quantum computations, is applied in this work.

In the ReaxFF concept, the overall potential energy E_p is formulated as a sum of partial energies which characterize the structure and state of the atomic system:

$$E_p = E_{bond} + E_{over} + E_{under} + E_{lp} + E_{val} + E_{tor} + E_{vdW} + E_{coul} + E_{ep} \quad (1)$$

Each term in Equation (1) corresponds to the energy contributions from: bonds (E_{bond}), over, and under-coordinated atoms (respectively: E_{over} , E_{under}) and lone pairs (E_{lp}). The E_{val} and E_{tor} denote energy contributions introduced by the valence and torsion angles. Terms E_{vdW} and E_{coul} are energies dependent on the non-bonded van der Waals and Coulomb interactions. The last term in (1), the penalty energy E_{ep} , controls the stability of the modelled system.

Depending on the type of atoms or molecules, additional components, like triple-bond energy correction (e.g. in the case of carbon monoxide) can be introduced to the total potential energy formulation.

Sets of fitting data are usually obtained on the basis of quantum computations and provided in a discrete tabularized form. In contrast to many other atomic potentials given in relatively simple mathematical expressions (like Stillinger–Weber model), the ReaxFF,

besides complex formulation, needs the interpolation of discrete data and routines like conjugated gradient-based charge-equilibration. All of these additional procedures make this approach computationally less effective than Stillinger–Weber and REBO (Mrozek, 2019) but at least allow the proper simulation of both 1T and 2H polymorphs without using *ab initio* computations. The data sets with parameters for SLMoS₂ used in this work were published by Ostadhossein et al. (2017).

4. Optimization problem formulation

The aim of optimization is to determine the values of the design variables describing the geometry of the nanostructure so that the mechanical properties of the obtained two-dimensional material are as close as possible to the set values. The nanostructure contains two-phases of MoS₂ and the share of each phase is defined with three variables, as shown in Figure 7.

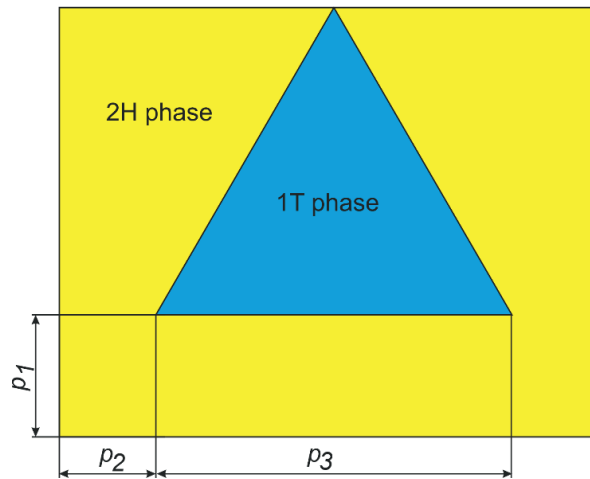


Fig. 7. The two-phase nanostructure with parameters defining both phases in unit cell

The design variables vector \mathbf{ch} contains coded values of parameters p_1 – p_3 . The objective function is defined as a norm of the difference of chosen material properties:

$$F(\mathbf{ch}) = \sum_{i,j} |C_{refij} - C_{ij}| \quad (2)$$

where C_{refij} is the reference value of stiffness matrix element ij and C_{ij} is the value of stiffness matrix element ij obtained for nanostructure defined by design variables vector \mathbf{ch} . The constraints are not imposed in the problem. The range of parameter values is defined by a number of bits and a coding algorithm. The objective function is computed on the base of the flowchart presented in Figure 8.

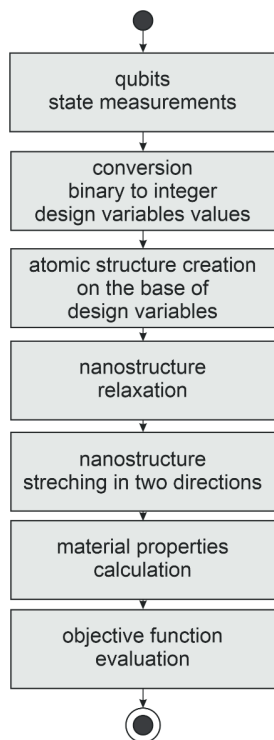


Fig. 8. The objective function evaluation on the base of qubits values

To determine the mechanical properties, it is necessary to perform numerical simulations with the use of molecular statics. During the simulation, the nanostructure is deformed and on the basis of the stress and strains values, it is possible to determine the components of its stiffness. Numerical simulations of the nanostructure were carried out using LAMMPS (Thompson et al., 2022) software, the ReaxFF (Aktulga, 2012) potential was used to simulate the interatomic interactions, which allows for the correct simulation of both phases and interactions between them in the MoS_2 material. The problem was coded with 12 qubits, each of the following 4 qubits corresponds to one of the variables describing the problem, Gray coding was used for the conversion from bit to an integer. After the measurements are made, the bits are converted into the values of the design variables. Design variables are used to build the nanostructure, which is then subjected to numerical analysis. As a result of the simulation, we obtain the mechanical properties of the nanostructure, which is used to calculate the value of the objective function.

5. Numerical examples

Two SLMoS_2 nanostructures containing two phases with substitute material properties close to the desired ones were generated as a result of the optimization. Figure 9

shows the first of the newly-created heterostructures. The boundaries of the lattice allow its periodic replication along the zigzag and armchair directions (compare with Figures 4 and 12). Mechanical material properties (components of the stiffness tensor) obtained during optimization (engaging molecular statics and ReaxFF potential), are close to the predefined ones and summarized in Table 1. Indices of the parameters C_{11} and C_{22} refer to the armchair and zigzag directions, respectively.

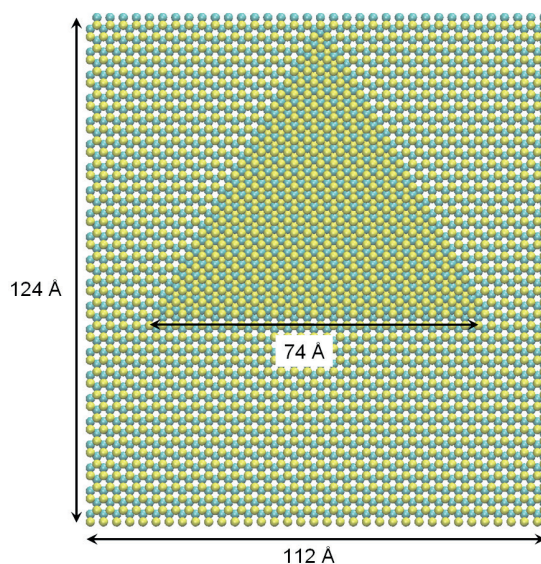


Fig. 9. The first of the generated 2H SLMoS_2 structures with triangular 1T inclusion

Table 1. Desired and actual properties of the structure from Figure 9 obtained during optimization

Parameter [GPa]	Predefined value	Actual value	Error [%]
C_{11}	130.0	129.5	0.4
C_{22}	110.0	114.7	4.3

The second example of optimized heterostructure, although similar to the previous one, is characterized by higher anisotropy. The main dimensions of the atomic model are shown in Figure 10, while its parameters are collected in Table 2.

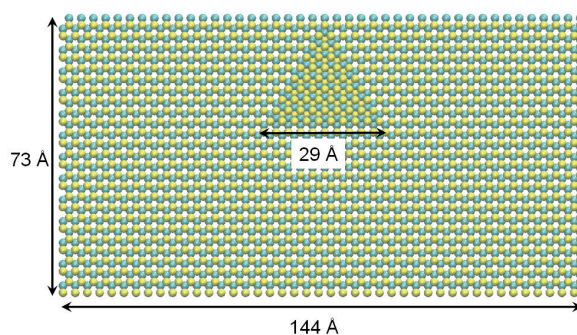


Fig. 10. The second of the optimized 2H SLMoS_2 structures with triangular 1T inclusion

Table 2. Desired and actual properties of the structure from Figure 10 obtained during optimization

Parameter [GPa]	Predefined value	Actual value	Error [%]
C_{11}	150.0	146.3	2.5
C_{22}	120.0	124.6	3.8

Mechanical properties

The following section describes the further, more detailed investigation of the two SLMoS₂ nanostructures, already obtained as an effect of quantum evolutionary optimization.

Mechanical properties and full stress-strain relations of obtained SLMoS₂ heterostructures at non-zero temperature were evaluated during the MD simulation of the tensile tests. The NPT ensemble with a pressure damping coefficient set to 100 fs and a time step equal to 0.25 fs was applied. Periodic boundary conditions were imposed along the zigzag and armchair directions.

The proposed simulation of the tensile test is based on the subsequent steps:

1. Pre-heating of the atomic model with a constant speed of 0.1 K/ps from 0 K to 30 K.
2. Relaxation of the unstrained nanostructure at 30 K.
3. Computation of the time-averaged micro-stress tensor σ using the virial theorem (Zhou, 2003):

$$\sigma = \frac{1}{\Omega} \sum_i^N \left[-m_i v_i \otimes v_i + \frac{1}{2} \sum_{j \neq i}^N r_{ij} \otimes f_{ij} \right] \quad (3)$$

where force f_{ij} , acting between atom i and j is computed as a derivative of the atomic potential energy E_p (using ReaxFF formulation, see Equation (1)), with respect to the distance vector r_{ij} (between the same considered atoms):

$$f_{ij} = - \frac{\partial E_p(r_{ij})}{\partial r_{ij}} \quad (4)$$

4. Computations of the time-averaged dimensions, the volume of the atomic system, and all other necessary quantities.
5. Imposition of the finite strain at the chosen direction.
6. Equilibration of the strained atomic lattice at 30 K.
7. Computation of the micro-stress tensor and the rest of time-averaged quantities (steps 3 and 4).

Steps 5–7 are repeated until a desired final strain or total failure of the structure is achieved. During the tensile test, models were stretched with the strain rate corresponding to the effective velocity of 10 m/s.

According to Shengping & Atluri (2004), the atomistic stress given by Equation (3) may be reduced to the Cauchy stress by neglecting the kinetic part and averaging the data necessary to obtain the stress tensor from each integration step over the time and geometry. A near-zero temperature of the simulation was chosen to keep the kinetic energy, and thus the vibrations of the atoms, at a low level. All data necessary to obtain stress-strain curves were averaged every 1000 time steps.

In the case of 2D materials such as graphene and SLMoS₂, it is more convenient to present the values of elastic constants and Young moduli in the force per length [N/m] units rather than common stress – force per area [GPa] units. It is mainly due to the problematic evaluation of the average effective thickness of the single atomic lattice. As reported by Narita et al. (2002), especially when a certain 2D material has many allotropes, the distance between two or more layers of atoms depends on the types of lattices and their mutual spatial orientation. The authors of this paper assumed the effective thickness of the SLMoS₂ lattices, as given by Jiang et al. (2013), equal to 6.092 Å, thus the results of the tensile tests are expressed in stress units.

The first considered example, the heterostructure obtained by the proposed quantum evolutionary optimization algorithm (as shown in Figure 9) has approximate dimensions of 112 Å × 124 Å and contains 4669 atoms. The side dimension of the triangular inclusion is equal to 74 Å. The obtained stress-strain relations are presented in Figure 11. The armchair and zigzag directions refer to the 2H surrounding area (see Figures 3 and 5 for details).

Unlike pristine 1T or 2H polymorphs, the investigated heterostructures reveal anisotropic properties. The average values of the Young moduli, roughly estimated on the initial parts (up to several percent) of the stress-strain graphs using linear regression, are equal to 133.4 GPa, and 123.6 GPa, respectively in the zigzag and armchair direction. These values are in good agreement with stiffnesses computed using molecular statics during optimization run (C_{11} and C_{22} , as presented in Table 1). For comparison: defectless 2H structures have a Young modulus in the range of 213 GPa ±50 GPa, while ideal 1T lattices – 91 GPa ±7 GPa. The exact values strongly depend on the method of investigation; see Mrozek (2019) for more details.

Regardless of the direction of the applied load, SLMoS₂ heterostructure starts to behave similarly when it is subjected to small deformations (i.e. 0–5%, neglecting slightly higher stiffness along a zigzag direction). The differences in the behaviour of the atomic model responsible for the failure mechanism begin to show under larger strains.

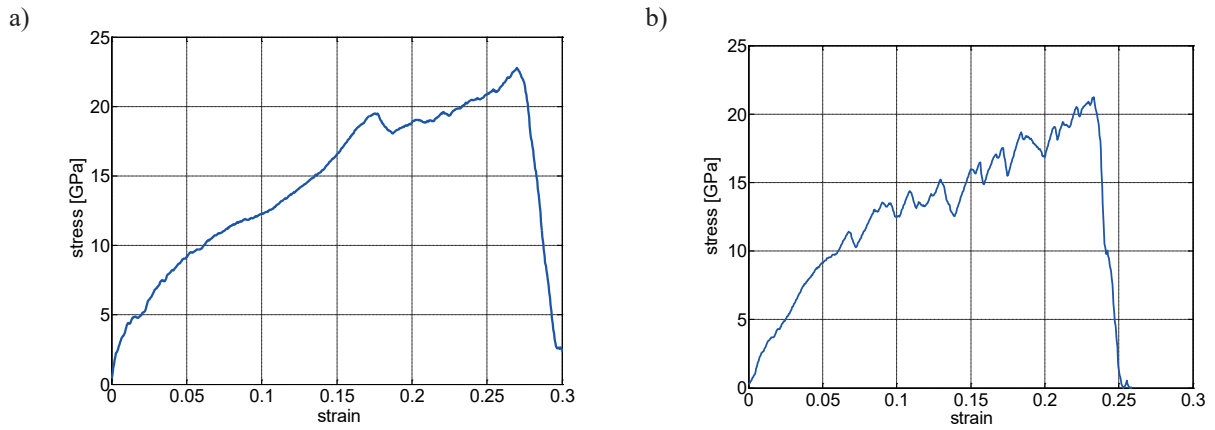


Fig. 11. Stress-strain relations of the first optimized structure: a) zigzag; b) armchair direction

As shown in Figure 12a, during the elongation of the lattice in the zigzag direction, the final damage is initiated by the movements of atoms in the privileged slip directions (see Figure 11a, approximately 18–26% of strain). The final failure (Fig-

ure 12b, strain >27%) starts, like the slips, from the tip of the 1T inclusion, however the particular place of the damage also depends on (random, but scale to the desired temperature) distribution of atom's initial velocities.

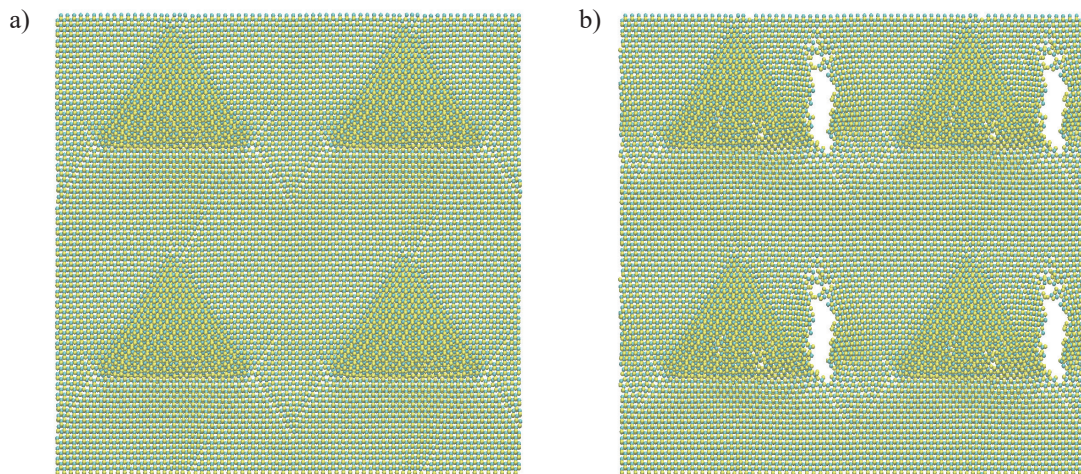


Fig. 12. Deformation of the heterostructure (replicated four times for better visualisation) along zigzag direction: a) slips; b) final damage

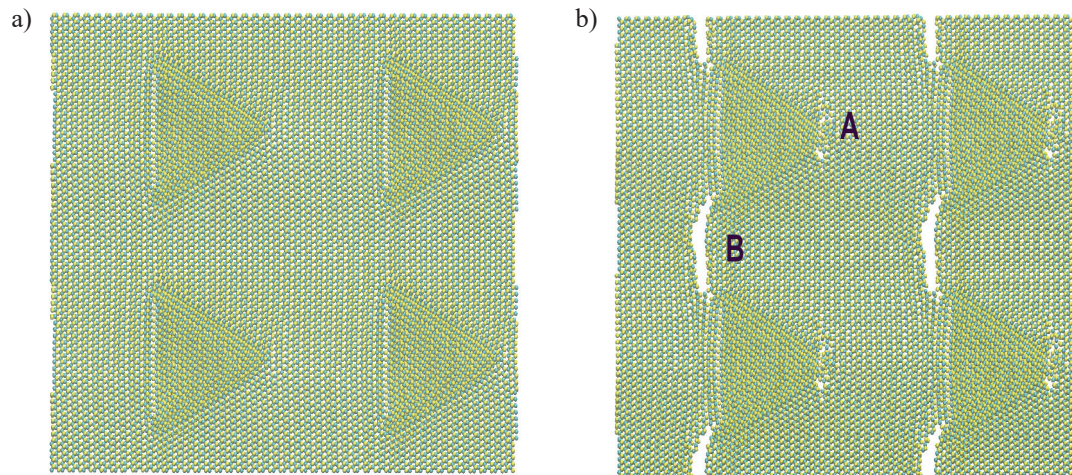


Fig. 13. Deformation of the heterostructure along armchair direction: a) elongated atomic bonds; b) final damage

In the case of armchair direction, slips in the 2H lattice do not occur. Instead of this, atomic bonds are elongated and softened (as presented in Figure 8a; approximately 12–20% of strain). Unlike the slip mechanism, in this case displaced atoms are unable to reach new equilibrium positions with a proper number of nearest neighbours. Elongated bonds tend to break, and atoms are attracted to one of the free boundaries. This phenomenon is responsible for the smaller ultimate strain during the tensile test in the armchair direction (23% vs. 27%).

The failure begins at the junction of the central tip of the inclusion with the rest of the structure (Figure 13b – A). Such an arrangement, where a small part of the triangular 1T lattice is surrounded from two sides by a large region of the 2H phase, results in many non-optimally bonded atoms, which can change their position easily during continuous deformation of the structure. In the next step (>23%), a crack is opened at the narrowest distance between two 1T phase inclusions (Figure 13b – B).

The second SLMoS_2 heterostructure, determined by the same optimization algorithm, contains 3371 atoms and has approximate dimensions equal to $144 \text{ \AA} \times 73 \text{ \AA}$ and the 1T inclusion has the shape of an equilateral triangle of dimension 29 \AA . Similar to the previous example, the armchair and zigzag directions refer to the rectangular 2H surrounding area. The obtained stress-strain curves are shown in Figure 14.

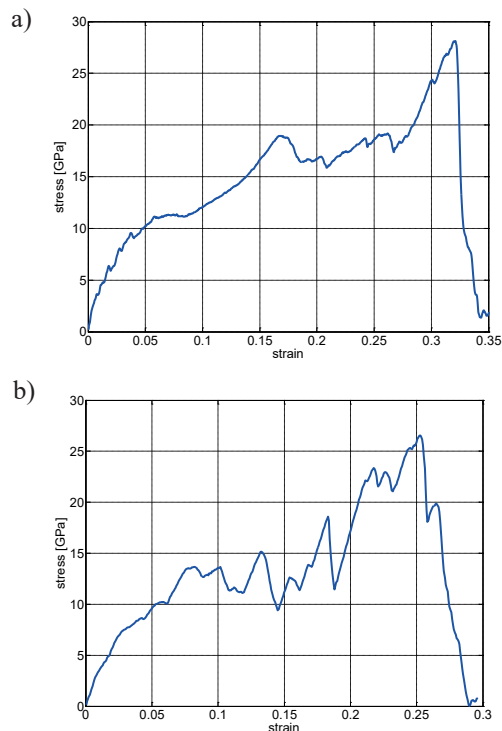


Fig. 14. Stress-strain relations of the second optimized structure: a) zigzag; b) armchair direction

In this example, estimated values of the Young moduli are respectively equal to 155.7 GPa in the zigzag direction, and 131.5 GPa along the armchair (compare with the stiffnesses collected in Table 2). The failure mechanisms which occurred in both directions are analogous to those described previously, however the increase in ultimate strengths and strains (as compared to the first example) are caused by the greater participation of the stiffer 2H phase.

6. Conclusions

The quantum-inspired evolutionary algorithm permits the solution of the optimization problem for two-phase heterogenous nanostructures. The objective function values were determined on the bases of Molecular Statics analyses in an atomic scale. The optimization problem was formulated as minimizing the difference between the given material parameters and the values for a given vector of design variables. The presented numerical example confirms that the proposed formulation of the optimization problem allows for structures to be obtained with a priori given material parameters.

Two cases of optimization with predefined mechanical properties were considered, and the algorithm allowed us to obtain the resulting nanostructures. The mechanical properties of the nanostructures were later confirmed using Molecular Dynamics simulations. The nanostructures behaviour up to the destruction strain have been presented and analysed.

The proposed method of heterogenous nanostructure optimization has been proven as a promising approach and can also be applied for other than SLMoS_2 materials in the future. The main drawback of the presented method is the computation time needed for analysis due to the atomic level simulations.

Acknowledgement

The research was funded by the National Science Centre, Poland, project no. 2021/43/B/ST8/03207. Calculations were performed in part at the Interdisciplinary Center for Mathematical and Computational Modeling, University of Warsaw, under grant GB80-16. We acknowledge EuroHPC JU for providing us with access to the Karolina supercomputer hosted by IT4Innovations, National Supercomputing Center, Ostrava, Czechia, under project 2010PA6018.

References

- Aktulga, H.M., Fogarty, J.C., Pandit, S.A., & Grama, A.Y. (2012). Parallel reactive molecular dynamics: Numerical methods and algorithmic techniques. *Parallel Computing*, 38(4–5), 245–259. <https://doi.org/10.1016/j.parco.2011.08.005>.
- Burczyński, T., Mrozek, A., Gorski, R., & Kus, W. (2010). Molecular statics coupled with the subregion boundary element method in multiscale analysis. *International Journal for Multiscale Computational Engineering*, 8(3), 319–330. <https://www.doi.org/10.1615/IntJMultCompEng.v8.i3.70>.
- Burczyński, T., Kuś, W., Beluch, W., Długosz A., Poteralski, A. & Szczepanik, M. (2020). *Intelligent Computing in Optimal Design*. Springer Cham, “Solid Mechanics and Its Applications” 261.
- Burczyński, T., Pietrzyk, M., Kuś, W., Madej, Ł., Mrozek, A., & Rauch, Ł. (2022). *Multiscale Modelling and Optimisation of Materials and Structures*. Wiley.
- Chenoweth, K., Duin, A.C.T. van, & Goddard, W.A. (2008). ReaxFF reactive force field for molecular dynamics simulations of hydrocarbon oxidation. *The Journal of Physical Chemistry A*, 112, 1040–1053. <https://doi.org/10.1021/jp709896w>.
- Cranford, S.W. & Buehler, M.J. (2011). Mechanical properties of graphyne. *Carbon*, 49(13), 4111–4121. <https://doi.org/10.1016/j.carbon.2011.05.024>.
- Duin, A.C.T. van, Dasgupta, S., Lorant, F., & Goddard, W.A. (2001). ReaxFF: A reactive force field for hydrocarbons. *The Journal of Physical Chemistry A*, 105(41), 9396–9409. <https://doi.org/10.1021/jp004368u>.
- Enyashin, A.N. & Ivanovskii, A.L. (2011). Graphene allotropes. *Physica Status Solidi B*, 248(8), 1879–1883. <https://doi.org/10.1002/pssb.201046583>.
- Han, K.H., & Kim, J.H. (2002). Quantum-inspired evolutionary algorithm for a class of combinatorial optimization. *IEEE Transactions on Evolutionary Computation*, 6(6), 580–593. <https://www.doi.org/10.1109/TEVC.2002.804320>.
- Jiang, J.W. (2015). Graphene versus MoS₂: a short review. *Frontiers of Physics*, 10, 106801. <https://doi.org/10.1007/s11467-015-0459-z>.
- Jiang, J.W., Park, H.S., & Rabczuk, T. (2013). Molecular dynamics simulations of single-layer molybdenum disulphide (MoS₂): Stillinger–Weber parametrization, mechanical properties, and thermal conductivity. *Journal of Applied Physics*, 114, 064307. <https://doi.org/10.1063/1.4818414>.
- Kandemir, A., Yapicioglu, H., Kinaci, A., Çağın, T., & Sevik, C. (2016). Thermal transport properties of MoS₂ and MoSe₂ monolayers. *Nanotechnology*, 27, 055703. <https://www.doi.org/10.1088/0957-4484/27/5/055703>.
- Kuś, W., Mrozek, A. & Burczyński, T. (2016). Memetic optimization of graphene-like materials on Intel PHI coprocessor. In L. Rutkowski, M. Korytkowski, R. Scherer, R. Tadeusiewicz, L.A. Zadeh, J.M. Zurada (Eds.), *Artificial Intelligence and Soft Computing. 15th International Conference, ICAISC 2016, Zakopane, Poland, June 12–16, 2016, Proceedings, Part I* (pp. 401–410). Springer Cham, “Lecture Notes in Computer Science” 9692. https://doi.org/10.1007/978-3-319-39378-0_35.
- Kuś, W., Akhter, M.J., & Burczyński, T. (2022). Optimization of monolayer MoS₂ with prescribed mechanical properties. *Materials*, 15(8), 1–9. <https://www.doi.org/10.3390/ma15082812>.
- Lahoz-Beltra, R. (2016). Quantum genetic algorithms for computer scientists. *Computers*, 5(24), 1–24. <https://doi.org/10.3390/computers5040024>.
- Li, H., Contryman, A.W., Qian, X., Ardakani, S.M., Gong, Y., Wang, X., Weisse, J.M., Lee, C.H., Zhao, J., Ajayan, P.M., Li, J., Manoharan, H.C. & Zheng, X. (2015). Optoelectronic crystal of artificial atoms in strain – textured molybdenum disulphide. *Nature Communications*, 6, 1–6. <https://www.doi.org/10.1038/ncomms8381>.
- Liang, T., Phillpot, S.R., & Sinnott, S.R. (2009). Parametrization of a reactive many-body potential for Mo–S systems. *Physical Review B*, 79(24), 245110. <https://doi.org/10.1103/PhysRevB.79.245110>.
- Liang, T., Phillpot, S.R., & Sinnott, S.R. (2012). Erratum: Parametrization of a reactive many-body potential for Mo–S systems. *Physical Review B*, 85(19), 199903(E). <https://doi.org/10.1103/PhysRevB.85.199903>.
- Lin, Y.C., Dumcenco, D.O., Huang, Y.S., & Suenaga K. (2014). Atomic mechanism of the semiconducting-to-metallic phase transition in single-layered MoS₂. *Nature Nanotechnology*, 9, 391–396. <https://www.doi.org/10.1038/nnano.2014.64>.
- Maździarz, M., Mrozek, A., Kuś, W. & Burczyński, T. (2018). Anisotropic-cyclicgraphene: a new two-dimensional semiconducting carbon allotrope. *Materials*, 11(3), 1–12. <https://doi.org/10.3390/ma11030432>.
- Mortazavi, B., Ostadhossein, A., Rabczuk, T., & Duin, A.C.T. van (2016). Mechanical response of all-MoS₂ single-layer heterostructures: a ReaxFF investigation. *Physical Chemistry Chemical Physics*, 18(34), 23695–23701. <https://doi.org/10.1039/C6CP03612K>.
- Mrozek A. (2019). Basic mechanical properties of 2H and 1T single-layer molybdenum disulfide polymorphs. A short comparison of various atomic potentials. *International Journal for Multiscale Computational Engineering*, 17(3), 339–359. <https://www.doi.org/10.1615/IntJMultCompEng.2019029100>.
- Mrozek, A. & Burczyński, T. (2013). Examination of mechanical properties of graphene allotropes by means of computer simulation. *Computer Assisted Methods in Engineering and Science*, 20(4), 309–323.
- Mrozek, A., Kuś, W. & Burczyński, T. (2010). Searching of stable configurations of nanostructures using computational intelligence methods. *Czasopismo Techniczne. Mechanika – Technical Transactions. Mechanics*, 107(20), 85–97.
- Mrozek, A., Kuś, W. & Burczyński, T. (2015). Nano level optimization of graphene allotropes by means of a hybrid parallel evolutionary algorithm. *Computational Materials Science*, 106, 161–169. <https://doi.org/10.1016/j.commatsci.2015.05.002>.
- Nakano, A. (1997). Parallel multilevel preconditioned conjugate-gradient approach to variable-charge molecular dynamics. *Computer Physics Communications*, 104(1–3), 59–69. [https://doi.org/10.1016/S0010-4655\(97\)00041-6](https://doi.org/10.1016/S0010-4655(97)00041-6).
- Narita, N., Nagai, S., Suzuki, S., & Nakao, K. (2000). Electronic structure of three-dimensional graphyne. *Physical Review B*, 62(16), 11146. <https://doi.org/10.1103/PhysRevB.62.11146>.

- Ostadhosseini, A., Rahnamoun, A., Wang, Y., Zhao, P., Zhang, S., Crespi, V.H., & Duin, A.C.T., van (2017). ReaxFF reactive force-field study of molybdenum disulfide (MoS_2). *The Journal of Physical Chemistry Letters*, 8(3), 631–640. <https://doi.org/10.1021/acs.jpcclett.6b02902>.
- Park, H., Fellingner, M.R., Lenosky, T.J., Tipton, W.W., Trinkle, D.R., Rudin, S.P., Woodward, Ch., Wilkins, J.W. & Hennig, R.G. (2012). *Ab initio* based empirical potential used to study the mechanical properties of molybdenum. *Physical Review B*, 85(21), 214121. <https://doi.org/10.1103/PhysRevB.85.214121>.
- Peng, Q., Ji, W. & De, S. (2012). Mechanical properties of graphyne monolayers: a first-principles study. *Physical Chemistry Chemical Physics*, 14(38), 13385–13391. <https://doi.org/10.1039/C2CP42387A>.
- Shen, S., & Atluri, S.N. (2004). Atomic-level stress calculation and continuum-molecular system equivalence. *CMES – Computer Modeling in Engineering & Sciences*, 6(1), 91–104. <https://doi.org/10.3970/cmcs.2004.006.091>.
- Silveira, L.R., da, Transcheit, R., & Vellasco, M.M.B.R. (2017). Quantum inspired evolutionary algorithm for ordering problems. *Expert Systems with Applications*, 67, 71–83. <https://doi.org/10.1016/j.eswa.2016.08.067>.
- Thompson, A.P., Aktulga, H.M., Berger, R., Bolintineanu, D.S., Brown, W.M., Crozier, P.S., Veld, P.J., in 't, Kohlmeyer, A., Moore, S.G., Nguyen, T.D., Shan, R., Stevens, M.J., Tranchida, J., Trott, C., & Plimpton, S.J. (2022). LAMMPS – a flexible simulation tool for particle-based materials modeling at the atomic, meso, and continuum scales. *Computer Physics Communications*, 271, 108171. <https://doi.org/10.1016/j.cpc.2021.108171>.
- Wang, Y., Lv, J., Zhu, L. & Ma, Y. (2010). Crystal structure prediction via particle-swarm optimization. *Physical Review B*, 82(9), 094116. <https://doi.org/10.1103/PhysRevB.82.094116>.
- Xiong, S., & Cao, G. (2015). Molecular dynamics simulations of mechanical properties of monolayer MoS_2 . *Nanotechnology*, 26(18), 185705. <https://doi.org/10.1088/0957-4484/26/18/185705>.
- Zhang, G. (2011). Quantum-inspired evolutionary algorithms: A survey and empirical study. *Journal of Heuristics*, 17(3), 303–351. <https://doi.org/10.1007/s10732-010-9136-0>.
- Zhou, M. (2003). A new look at the atomic level virial stress: on continuum-molecular system equivalence. *Proceedings of the Royal Society A*, 459(2037), 2347–2392. <https://doi.org/10.1098/rspa.2003.1127>.

